Received: 1 March 2022 | Revised: 22 August 2022 | Accepted: 23 September 2022

DOI: 10.1002/suco.202200204

ARTICLE

fib CEB-FIP WILEY

Experimental methods for the analysis of the durability behavior of concrete joints

Jan P. Höffgen[1] | **Matthias Mohs**[1,2] | **Sarah Lamparter**[1] | **Viktória Malárics-Pfaff**[2] | **Frank Dehn**[1]

[1]Institute of Concrete Structures and Building Materials, Karlsruhe Institute of Technology, Karlsruhe, Germany

[2]Federal Waterways Engineering and Research Facility, Structural Engineering, Karlsruhe, Germany

Correspondence
Jan P. Höffgen, Institute of Concrete Structures and Building Materials, Karlsruhe Institute of Technology, Gotthard-Franz-Str. 3, Karlsruhe 76131, Germany.
Email: jan.hoeffgen@kit.edu

Funding information
Federal Ministry for Digital and Transport: BMVIExpertennetzwerk Wissen - Können - Handeln, Grant/Award Number: B3951.03.04.70014

Abstract

This article addresses the applicability of experimental methods for the evaluation of concrete durability on localized structural weaknesses posed by joints. Three different types of exposure are analyzed: chloride penetration, carbonation, and freeze–thaw attack. First, established experimental methods for the characterization of the durability of plain concrete are presented and their general applicability on concrete joints is discussed. The experimental program focuses on the execution of selected tests on laboratory specimens with and without joints. Indicator tests for both chloride penetration and carbonation are generally feasible, but require attention to specimen preparation. Rapid chloride migration yielded inconclusive results, while uniaxial chloride diffusion coefficient of concrete joints cannot be determined because of the areal extent of profile grinding. For the same reason, the characterization of the resistance to freeze–thaw cycles through surface deterioration is not applicable for concrete joints. The structural damage was instead successfully qualified through direct tension tests.

KEYWORDS

carbonation, chloride diffusion, concrete durability, direct tension test, freeze–thaw resistance, joint, plain concrete, RCM

1 | INTRODUCTION

The design concept for durable concrete structures distinguishes between two general damage mechanisms: corrosion of reinforcement and corrosion of concrete. The former can be caused by carbonation of the alkaline components of the hardened cement paste in the surrounding concrete or due to chloride penetration. Concrete corrosion may have diverse causes, such as solvent (e.g., soft or acidic water), expansive (e.g., sulfates or alkali-silica-reaction), mechanical (e.g., abrasion), and physical attack (e.g., freeze–thaw action). The resistance to both, however, is mainly formed by the properties of the surrounding concrete. The encompassing parameters for all corrosive attacks are concrete capillary porosity, as

Discussion on this paper must be submitted within two months of the print publication. The discussion will then be published in print, along with the authors' closure, if any, approximately nine months after the print publication.

corrosion resistance declines with higher capillary pore volume and diameters, as well as concrete diffusivity. The descriptive design concept found in EN 206:2017-01[1]; therefore, defines concrete requirements such as lower boundaries for compressive strength and cement content and an upper boundary of water to cement (w/c)-ratio, depending on the mechanism and magnitude of the corrosive attack.

While the descriptive design concept generally allows for durable concrete structures, discontinuities such as concrete joints are not accounted for in building codes.

In principle, concrete joints are structural weaknesses, which however cannot be omitted in the design of structures with large dimensions. The reason for this lies in the production process. When casting a single layer of concrete, the local composition at the edges differs from the bulk material due to segregation or wall effects, resulting in a locally increased paste content, w/c-ratio, and porosity, which is further enhanced in case of insufficient compaction or curing.[2,3] When adding a second layer of concrete, the forming bond is strongly affected by the surface quality of the first layer. This effect can be mitigated by removing the impaired peripheral concrete before the formation of the joint.[4,5] Even so, joints are also prone to cracking for their low tortuosity compared with monolithic concrete, where crack paths deviate due to coarse aggregate distribution. Nonetheless, the assessment of concrete joint durability has not been widely regarded in past research. In repair and retrofitting, joints are seen as durable as long as their adhesive bond strength is sufficiently high, subsequently neglecting arising questions of corrosion mechanisms. Past research has focused on crack development over time, or debonding, and its influencing factors,[6,7] with special consideration of differential shrinkage[8–10] and freeze–thaw cycles (FTC).[11–15] The effect of concrete joints on carbonation and chloride diffusion, however, has so far only received marginal attention.[16–18] Additionally, the durability of concrete repair was found to be influenced by surface contamination prior repairing.[19–23] This issue, with few exceptions,[24,25] does not regard the influence of concrete joints acting as pathways for water and other harmful substances, which is the case, for example, for hydraulic structures, where joints are required for the sectional construction method. Past research, however, highlight the need for specialized test setups when investigating durability of concrete joints.

This article focuses on three of the main durability issues—chloride diffusion, carbonation, and freeze–thaw attack—and the application of established test methods for quantifying the influence of joints on the durability of concrete structures.

2 | PROCEDURES FOR THE ANALYSIS OF CONCRETE DURABILITY

2.1 | Chloride penetration

Chlorides can be present in concrete through external supply, that is, in form of thawing agents or marine salts or contribution by concrete ingredients. They are not problematic for the concrete itself but may act as trigger for a local depassivation of the reinforcement when dissolved in pore solution. During hydration of Portland cement, chlorides are physically or chemically bound to C-S-H and aluminous phases. Chlorides from external supply can, to a smaller degree, be bound physically or chemically as well. Excess chlorides remain dissolved and may be transported into deeper concrete layers through convection and diffusion.[26]

Chloride penetration tests can be classified as long-term diffusion and short-term migration tests. Short-term migration tests exploit that chloride-ion movement in a fluid can be accelerated through electric fields. The rapid chloride migration (RCM) test setup positions a water-saturated cylindrical concrete specimen between a hydroxide solution and a hydroxide-chloride solution. An electric field forces the chlorides to migrate through the specimen. After a determined test duration t in [h], the specimen is recovered, cracked, and treated with a silver nitrate solution for measuring the mean chloride penetration depth x_d in [m]. The chloride migration coefficient is calculated from Equation (1) by factoring in the mean temperature T in [K] of the test solution, specimen height h in [m], and applied voltage U in [V], according to BAW-Code of Practice MDCC.[27] Adaptions of Equation (1) are necessary when altering the test solutions.

$$D_{RCM} = \frac{2.39 \times 10^{-8} \times T \times h}{(U-2) \times t} \times \left(x_d - 0.0236 \times \sqrt{\frac{T \times h \times x_d}{U-2}} \right) \left[\frac{m^2}{s} \right] \quad (1)$$

The RCM-test can be easily adopted for evaluating concrete joints, which need to be arranged parallel to the direction of chloride migration and predefine the subsequent cracking. An alternative to RCM is the rapid chloride penetration test, which differs especially through higher voltage, chloride concentration, and shorter test duration.[28] Long-term uniaxial diffusion test specimens according to EN 12390-11:2015-11[29] are vacuum-saturated with water, sealed with the exception of one front surface, stored in a saturated $Ca(OH)_2$-solution for

18 h, and subsequently submerged in a chloride solution. Other test setups like the salt ponding test[30] or the bulk diffusion test[31] use different chloride solution exposure methods and concentrations, but also rely on diffusion and, to a lesser degree, convection as the main chloride transport mechanisms. Other varying parameters are the composition of the chloride solution and the duration of the exposure. For test evaluation, the amount of acid-soluble chlorides is measured on concrete powder samples received from grinding several layers parallel to the exposed surface. The chloride diffusion coefficient can subsequently be determined by fitting a Gauss error function (as the solution of Fick's second Diffusion Law differential equation) to the chloride profile, which has to be corrected for the initial chloride content obtained from an unexposed reference specimen.

Since profile grinding requires an area that is much larger than the narrow band of a concrete joint, the determination of the chloride diffusion coefficient is not reasonable. A qualitative analysis can, however, follow the evaluation of RCM-test by measuring the chloride penetration depth x_d through the silver nitrate indicator test.

2.2 | Carbonation

Without the exposure to catalysts like chlorides, concrete reinforcement is protected from corrosion through passivation. In an alkaline environment with pH > 11, steel forms a dense oxide layer, which prevents further corrosion. Due to the formation of calcium hydroxide ($Ca(OH)_2$) during the hydration of cement and other alkalis (KOH, NaOH) in the pore solution, the pH value of concrete is around 13. Carbon dioxide (CO_2), which diffuses into the concrete through capillary pores, may ultimately react with calcium hydroxide and form calcium carbonate. This lowers the pH value below 9, resulting in a depassivation of reinforcement.[26,32]

The assessment of concrete carbonation resistance follows a general procedure: After exposure to a specific concentration of CO_2, a concrete specimen is cracked perpendicular to the exposed surface. The freshly broken crack surfaces are treated with a phenolphthalein solution, which stains areas with pH >8.2–9.8 violet. Treatment has to occur immediately after cracking, lest crack surfaces start to carbonate. The carbonation depth is subsequently measured and, using the $\sqrt{t}-$law, carbonation rate or the inverse carbonation resistance can be calculated.

Variations of the test procedure include relative humidity (r.h.) and CO_2-concentration, enabling accelerated testing. Fib Bulletin 34[33] calculates the inverse effective carbonation resistance $R^{-1}_{ACC,0}$ of a concrete specimen after being exposed to an elevated CO_2-concentration ΔC_s in [kg/m^3] using the carbonation depth x_c in [m] resulting from an exposure for a duration t in [s] (Equation 2).

$$R^{-1}_{ACC,0} = \left(\frac{x_c}{\sqrt{2 \times \Delta c_s \times t}}\right)^2 \left[\frac{m^2}{s} / \frac{kg}{m^3}\right] \quad (2)$$

The phenolphthalein indicator test can be easily adopted for the evaluation of concrete joints, which predetermine the crack path, and no adaptions are required.

2.3 | Freeze–thaw attack

When concrete is subjected to low temperatures causing water in pores to freeze, the accompanying increase in water volume may result in microstructural damage. Crucial influencing factors are capillary porosity and water saturation as well as the frequency and magnitude of low temperatures. Frost damage requires saturated concrete, where freezing water cannot expand into empty pore space. Unsaturated concrete is less prone to frost damage, but shows significant cryogenic suction in case of an external water supply due to the influence of pore diameter on the freezing point of pore water. This results in a growing water saturation with lower temperatures and repeated FTC, and subsequent frost damage.[26,34–37]

The experimental assessment of the freeze–thaw resistance of plain concrete focuses on two parameters: surface deterioration and internal structural damage. Variations of test procedures include the attacking medium (deionized water/deicing-salt solutions), interval (continuous/during thawing), and direction (one-sided/all-sided) as well as specimen geometry and preparation. Due to ongoing freezing and thawing, a surface in contact with water will develop microcracks, which subsequently merge into larger cracks beginning at the exterior specimen sides and cause exposed surfaces to deteriorate. Standards like CEN/TS 12390-9[38] classify concrete resistance through the measurement of specimen mass loss per unit area and a set number of FTC with predefined time–temperature-curves. Deterioration resulting of one-sided exposure can be used for the assessment of concrete surface quality and preparation methods. However, since concrete joints only constitute a narrow band of the exposed surface, this procedure is not suited for the assessment of joint durability itself.

The internal structural damage can be assessed through a number of procedures. CEN/TR 15177:2006-06[39] describes the execution of length change tests and relative dynamic modulus of elasticity

tests. Microcracks result in specimen expansion due to the creation of voids. When these microcracks are distributed evenly over a specimen, the total expansion becomes quantifiable through intermittent measurements after set numbers of FTC. Since a joint only affects a small proportion of a specimen, deformations of the joint are small compared with the overall deformations and can only be measured with additional expense, thus rendering this procedure unsuited. The assessment of the relative dynamic modulus (RDM) of elasticity, which is also standardized in CEN/TR 15177:2006-06,[39] faces similar problems, but is expected to be more sensitive to concentrated cracks at the joint than the measurement of length changes. RDM is obtained from ultrasonic pulse measurements following Equation (3), where $t_{S,n}$ in [s] is the ultrasonic transition time after n FTC. Alternatively, RDM is the squared quotient of the fundamental transverse resonant frequencies after/before FTC.

$$\mathrm{RDM_n} = \left(\frac{t_{S,0}}{t_{S,n}}\right)^2 \quad [-] \tag{3}$$

In addition to these standardized procedures, internal structural damage can be assessed through tensile tests. The tensile behavior of concrete is prone to cracks, but its determination is time-consuming, especially in case of direct tensile tests. However, when tensile strength and tension softening are already important material parameters, which is the case for concrete joints, tensile tests can provide valuable results.[40,41]

3 | SPECIMEN PREPARATION AND TEST EXECUTION

3.1 | Concrete casting and strength testing

All specimens for the experimental analysis were produced in six casting batches. Aggregates were quartzitic Rhine sand and Rhine gravel with AB16 as grading curve. CEM I 32.5 R was used as binder with a water/cement-ratio of 0.50. Table 1 shows the adopted mix design.

Specimens were cast in steel molds with spacers for allowing the addition of a second concrete layer. Two joint preparation methods were adopted: as-cast (a), where joints were left untreated after smoothing with a trowel, and water-jetted (w), where the surface of the old concrete was roughened with a hand lance at 220 bar, 24 h after mixing, as well as monolithic specimens (m) without joints for reference and strength testing. Joints were generally produced horizontally at medium specimen height. Storage between demolding and the addition of the second concrete layer at the age of 7 days varied depending on the investigated parameters.

TABLE 1 Mix design for laboratory analysis

		Proportion [kg/m³]
Sand	0–2 mm	669
Gravel	2–8 mm	362
Gravel	8–16 mm	777
CEM I 32,5 R		350
Water		170
Super plasticizer		5.3

Monolithic specimens for strength tests were moist-stored under wet burlap at 20°C for 7 days after mixing and dry-stored at 65% r.h. and 20°C until testing. Extensive strength tests were performed on one batch, yielding the results in Table 2. The average cube compressive strength for all batches was $f_{cm,cube,28days} = 57.0$ MPa.

3.2 | Chloride penetration

Specimens for chloride penetration tests were continuously stored under water at 20°C. At the age of 7 days of the first layer, specimen halves were taken from the water bath some time before the concreting of the second layer, allowing the joint surface to superficially dry. Before testing, drill cores with a diameter of $d = 100$ mm and a height of $h = 50$ mm were extracted from cubes, so that the joint was perpendicular to the circular cross-section (see Figure 1).

At the age of 28 days of the second layer, chloride penetration tests were initiated. Specimens for RCM-testing were used without further preparation, whereas lateral surfaces and one front surface of cylinders for unidirectional diffusion tests were sealed with epoxy resin. Specimens for unidirectional diffusion tests were submerged in a 3% NaCl solution for 90 days according to EN 12390-11:2015-11.[29] 0.2 N KOH and 0.2 N KOH +- 10% NaCl solutions were used for RCM-tests at 25 V for 24 h.[27] The alterations provided by EN12390-18:2021-09[42] were issued during the evaluation of the test results and were therefore not included in the presented analysis.

3.3 | Accelerated carbonation

Specimens for accelerated carbonation tests were produced in the same manner as for chloride testing, except

those cubes with l = 100 mm were used. Specimens were stored at 20°C under wet burlap between the casting of the first and second layer and the subsequent 7 days. A second series of carbonation tests switched the storage under wet burlap with water-storage. Afterwards, specimens were dry-stored at 65% r.h. and 20°C. At the age of 28 days of the second layer, the specimens were exposed to 3 vol.% CO_2, at 65% r.h. and 20°C.

TABLE 2 Results of the accompanying compressive and tensile splitting strength tests on monolithic cubes with $l = 150$ mm and cylinders with $d = 300$ mm at the age of 28 and 56 days according to EN 12390-3:2019-10[45]; EN 12390-6:2010-09[46]; EN 12390-13:2014-06[47]

		28 days	56 days
Compressive strength	Cube [MPa]	57.5	60.4
Compressive strength	Cyl [MPa]	48.3	52.6
Elastic modulus	Cyl [GPa]	33.4	33.2
Tensile splitting strength	Cyl [MPa]		3.6

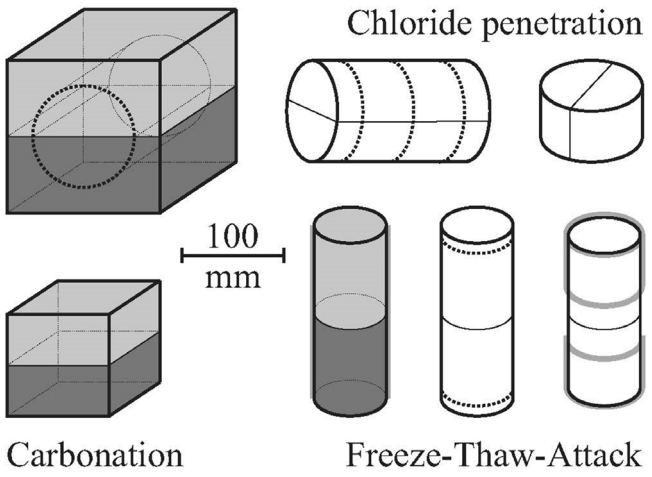

FIGURE 1 Schematic presentation of jointed specimen preparation for chloride penetration, carbonation, and freeze–thaw tests.

3.4 | Freeze–thaw resistance

In order to use the same specimens and to enable the inclusion of joints for the measurements of the relative dynamic modulus and direct tensile tests after exposure to FTC, the test method from CEN/TR 15177:2006-06[39] was adapted to meet the diverse requirements.

Cylindrical specimens with a diameter of $d = 71$ mm and a total height of $h = 150$ mm were cast in polypropylene tubes, which were cut open for demolding in order to avoid the use of release agents. After casting the first layer and for one additional day after adding the second concrete layer, tubes were covered with wet burlap at 20°C, followed by storage under water for 6 days and subsequent dry-storage at 65% r.h. and 20°C. At the age of 28 days of the second layer, cylinders were sealed with epoxy resin, baring a stripe with a width of 50 mm around the joints, thus reducing the risk of surface deterioration of the front faces. Specimens were subsequently subjected to 0, 14, 28, or 56 FTC starting individually so that the ultimate FTC ended 56 days after producing the second specimen layer. One FTC took 12 h with maximum and minimum temperature being 20 and −20°C, respectively, corresponding to CEN/TR 15177:2006-06.[39] For enabling RDM measurements after set numbers of FTC, flooding was reduced to every other cycle.

As the joints provide a structural weakness, which localizes cracking, deformations w could be measured with three inductive displacement sensors and a measuring length of $l_0 = 50$ mm. For predefining crack initiation in monolithic cylinders, a notch with a depth of 5 mm had to be cut into each specimen. This was carried out after the final FTC so that the surface was always the same size during the FTC. Before starting the deformation-controlled tensile test, each specimen was

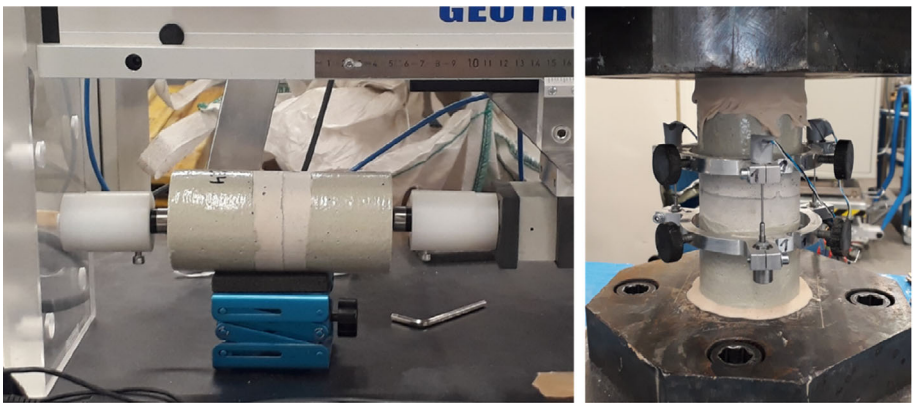

FIGURE 2 Experimental assessment of the structural damage after freeze–thaw attack left: Relative dynamic modulus measurement, right: direct tension test.

Joint type	d_c [mm]	D_{RCM} $\left[10^{-11}\frac{m^2}{s}\right]$	$R^{-1}_{ACC,0}$ $\left[10^{-11}\frac{m^2}{s}/\frac{kg}{m^3}\right]$
Monolithic	16.2 ± 0.5	1.36 ± 0.20	17.2 ± 2.0
Water-jetted	15.3 ± 0.9	1.30 ± 0.06	30.7 ± 7.5
As-cast	15.2 ± 0.9	1.21 ± 0.08	60.2 ± 33.1

TABLE 3 Results of unidirectional chloride diffusion (d_c), rapid chloride migration (D_{RCM}) and accelerated carbonation test ($R^{-1}_{ACC,0}$)

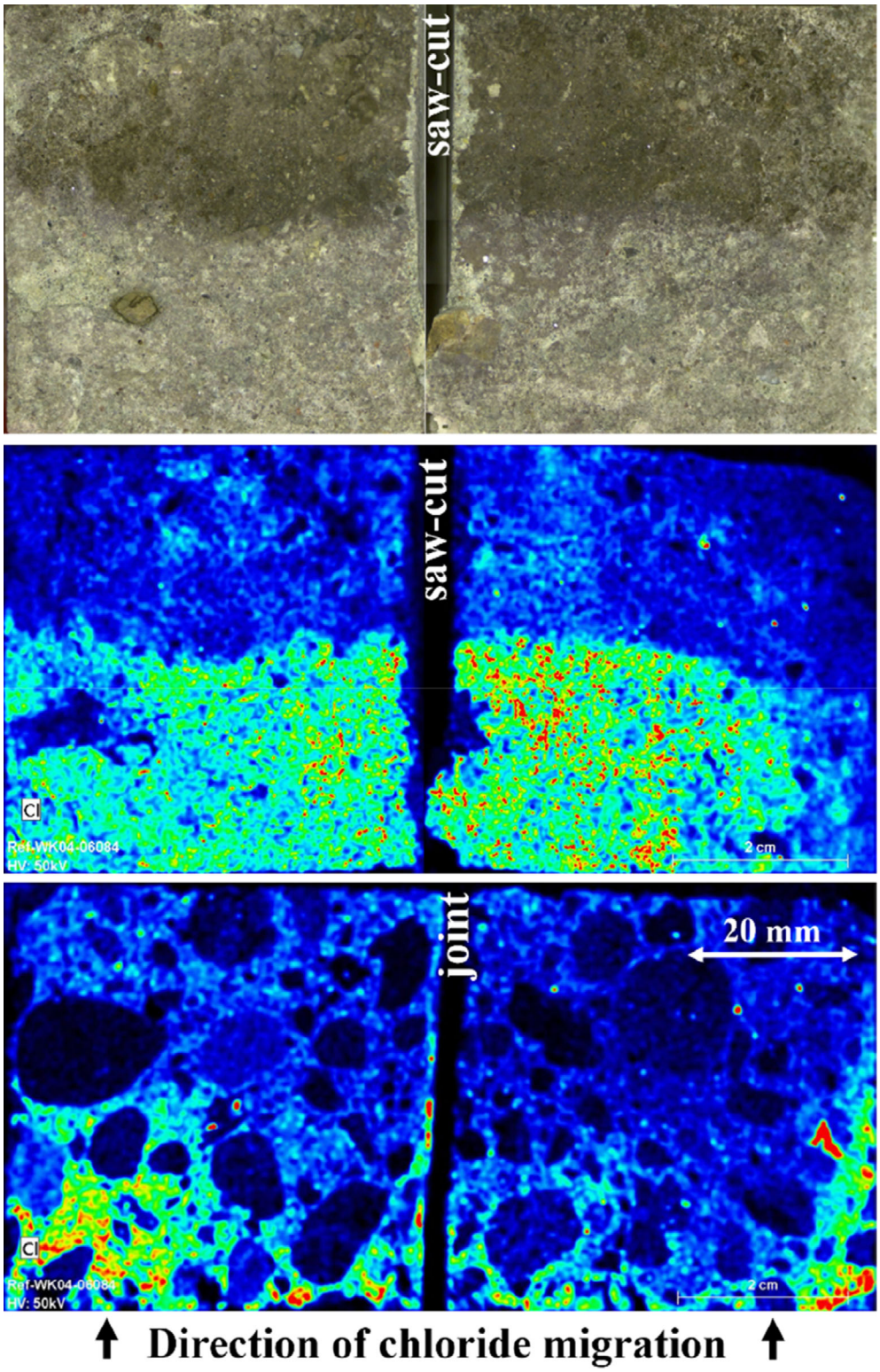

FIGURE 3 Relative chloride concentration following rapid chloride migration in micro-XRF test on a specimen with as-cast joint. Top: Visualization of the chloride penetration depth through the silver nitrate indicator test, mid: Corresponding micro-XRF image of the joint surface, bottom: micro-XRF image of saw-cut surface. Relative cl^--concentration rising from blue over green to red.

glued to the load application panels with a fast-setting two-component adhesive and left to harden for 20 min. Deformation was then applied with a strain rate of $\frac{dw}{dt} \cdot \frac{1}{l_0} = \dot{\varepsilon} = 1 \cdot 10^{-5}\ \mathrm{s}^{-1}$. Tensile forces F_t and deformations w were recorded at 25 Hz. Test execution of RDM and direct tension is depicted in Figure 2.

For the description of tensile behavior, three characteristic parameters were analyzed: (net) tensile strength f_{ct}, secant modulus of elasticity $E_{ct,S}$, and fracture energy G_F as well as a linearity coefficient L describing the ratio of two secant moduli determined for $\sigma_a = \frac{1}{3} \cdot f_t$ and $\sigma_a = \frac{1}{6} \cdot f_t$, respectively.[43]

4 | RESULTS OF THE EXPERIMENTAL ANALYSIS

4.1 | Chloride penetration

Measurements of chloride penetration depth could be carried out as expected. Table 3 indicates results of unidirectional chloride diffusion and RCM tests. Differences between joint types were marginal. Monolithic concrete performed slightly worse than concrete joints, illustrated by higher values of d_c and D_{RCM}.

For validating the measurements of chloride penetration depth through silver nitrate indicator testing, additional micro-X-ray fluorescence (XRF) tests were conducted on selected specimens after RCM-testing. In addition to the qualitative determination of the chloride distribution in the joint, specimens were dry-sawn perpendicular to the joint, thus allowing the assessment of the chloride distribution in the joint and the bulk concrete of the same specimen. Figure 3 shows an exemplary result of a specimen with an as-cast joint.

Due to imperfect sealing at the outer edges, chlorides can migrate from two directions into the specimen, which results in a higher chloride concentration in the bulk concrete that needs to be neglected. Micro-XRF shows a nearly constant chloride profile in the joint for the area underneath the chloride penetration front identified through the silver-nitrate indicator test (Figure 3). For the bulk concrete, on the other hand, a chloride gradient can be identified. Although the penetration depth obtained from silver-nitrate indicator tests appears not to be influenced by joints, micro-XRF raises questions regarding the evaluation method due to differing chloride distribution. An extensive micro-XRF analysis, however, requires an initial calibration for converting relative chloride distributions into quantitative chloride content.[44]

4.2 | Carbonation

After exposure to CO_2 for 28 days, specimens were split in the plane of the joint and the depth of the carbonation

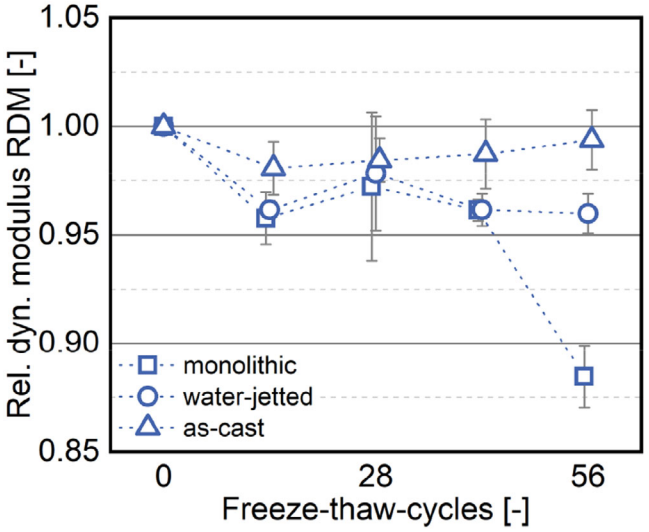

FIGURE 5 Development of the average relative dynamic modulus (RDM) from 0 to 56 freeze–thaw cycles.

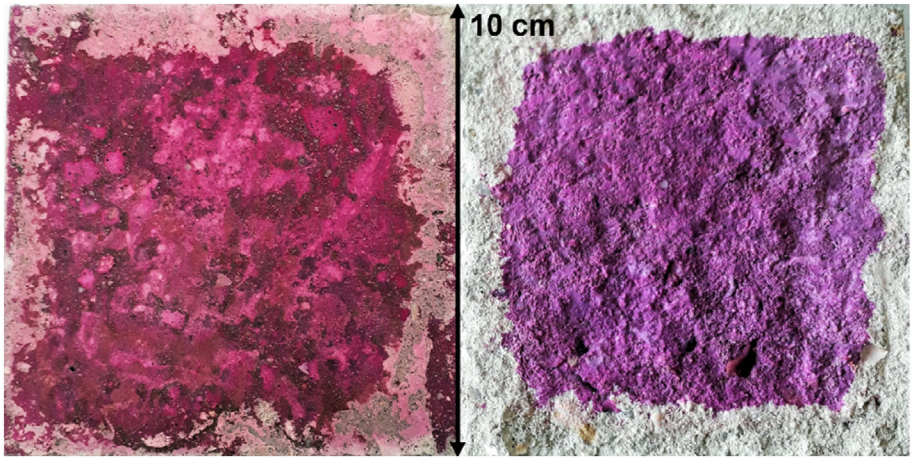

FIGURE 4 Phenolphthalein indicator test on carbonated interfaces with as-cast joints. Left: Storage under wet burlap sacks, right: Storage under water before the addition of the second concrete layer.

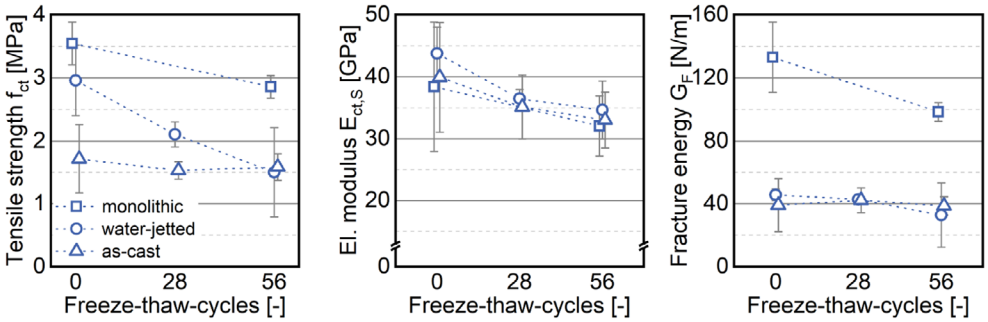

FIGURE 6 Average tensile strength f_{ct} (left), secant modulus of elasticity $E_{ct;S}$ (mid), and specific fracture energy G_F (right).

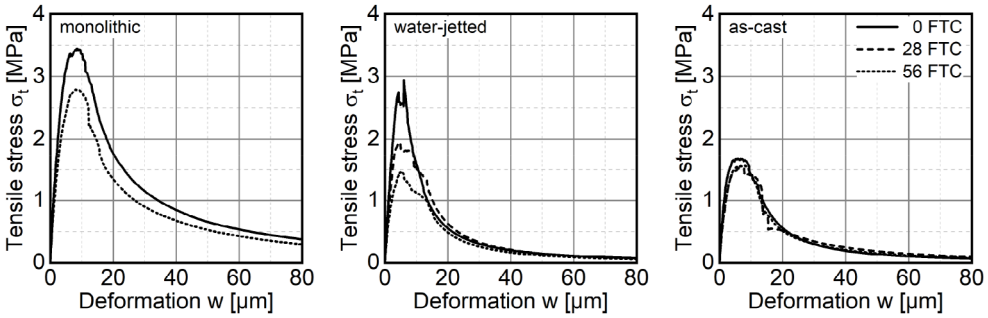

FIGURE 7 Average tensile-stress-deformation curves for different numbers of freeze–thaw cycles (FTC) and joint preparation methods (left: monolithic, mid: water-jetted, and right: as-cast).

front was made visible through the color change of the phenolphthalein solution. Thus, it was possible to measure the depths of the color change at 24 points and averaging them.

The initial results of phenolphthalein indicator tests underline the importance of specimen storage between the casting of the first and second layer. Specimens, where the first half was stored under water, show a clear color change indicating the carbonation depth. When the first concrete layer was stored under wet burlap, the phenolphthalein indicator test did not yield usable results. Apparently, the high relative humidity did not fully prevent carbonation of the joint interface before the casting of the second layer. The indicator test therefore did not yield a clear color change, which is illustrated in Figure 4.

Joints simplify measurements for their lack of coarse aggregate when compared with monolithic concrete. Subsequently calculated inverse effective carbonation resistance is shown in Table 3. $R^{-1}_{ACC,0}$ for joints is 1.8 to 3.5 times higher than for monolithic concrete, thus stressing the need for further research.

4.3 | Freeze–thaw attack

The initial measurements of the dynamic modulus of elasticity at the age of 28 days yielded no significant influence of joints ($E^{m}_{dyn,28days}$ = 40.6 (14) GPa, $E^{w}_{dyn,28days}$ = 40.8 (8) GPa, $E^{a}_{dyn,28days}$ = 40.2 (11) GPa). Figure 5 shows the development of RDM for specimens with up to 56 FTC. With one exception RDM of all series remain in a narrow band between 0.95 and 1.00 after an initial drop between 0 and 14 FTC. Remarkably, monolithic specimens show the lowest measured values of RDM and a significant drop between 42 and 56 FTC. The cause for this behavior was not investigated within the scope of this article. Standalone RDM measurements do not suffice for the assessment of the freeze–thaw behavior of concrete joints but require additional consideration of the moisture content for predicting similar damage progress compared with splitting tensile tests.[14]

In contrast to RDM, present tensile tests show an influence of FTC and joint preparation. Although a considerable amount of damaged material is removed by the notch, Figure 6 shows that both tensile strength f_{ct} and specific fracture energy G_F of monolithic concrete decline after exposure to FTC. This affirms the hypothesis that tensile tests are suitable for quantifying internal structural damage. Even the secant moduli $E_{ct,S}$ of specimens subjected to FTC are lower than compared with the reference, despite being distorted by the notch.

As-cast joints show a lower initial tensile strength and specific fracture energy when compared with monolithic concrete. The secant modulus of elasticity is higher because of the neglection of the notch for the calculation of $E_{ct,S}$. Water-jetting has a positive impact on tensile strength and secant modulus of elasticity by removing weak concrete near the interface, but does not roughen

the surface and therefore leaves fracture energy almost unchanged when compared with as-cast joints.

FTC generally affect concrete tensile behavior, although the effects vary depending on joint execution. In monolithic concrete, structural damage appears in a reduced tensile strength, secant modulus of elasticity and fracture energy. The decrease of tensile strength is also present in water-jetted joints, whereas fracture energy appears to be unaffected. Stress-deformation curves illustrate this behavior in form of a capped stress-peak and nearly identical tension-softening (Figure 7). The secant modulus of elasticity declines in a similar magnitude regardless of specimen type. The linearity coefficient reduces from 94% to 81% for notched monolithic specimen, from 95% to 84% for specimen with water-jetted joints and from 89% to 86% for as-cast joints. Apart from that, as-cast joints show no significant changes of tensile strength nor fracture energy.

5 | CONCLUSION

This article shows that many experimental methods to evaluate concrete durability are not practicable for the assessment of concrete joints due to being localized structural weaknesses. This holds true especially for the determination of chloride profiles from ground powder and length changes due to internal structural damage that is, caused by FTC.

An alternative to the former provides the silver nitrate indicator test on concrete surfaces, which need to be obtained by cracking along the joint. This provides qualitative results in comparison to monolithic concrete. The present research yielded no negative impact of concrete joints on chloride penetration depth, arising questions regarding the applicability of the determination of chloride penetration through silver nitrate. The indicator tests deliver only the penetration depth for a single chloride concentration. For a quantitative assessment of chloride diffusion, the shape of the chloride profile is equally important. Micro-XRF allows for the visualization and assessment of different chloride distributions of the joint and bulk concrete of a single specimen. The determination of chloride diffusion coefficients from micro-XRF is not standardized but feasible with the inclusion of additional experiments for calibration.

The indicator test for measuring carbonation depth, on the other hand, proved to be feasible and inexpensive, as it directly correlates with the depassivation depth for reinforcement corrosion. Limitations involve the joint preparation prior to casting the second layer: Interfaces in contact with air or CO_2, respectively, tend to carbonate superficially before the addition of an additional layer of concrete, thereby rendering the indicator test prone to errors. This may even impede the testing of specimens extracted from existing structures. The presented results, where the exposure to CO_2 during the specimen production process was prevented by water-storage, show a great negative impact of concrete joints on carbonation resistance.

Measurements of the relative dynamic modulus of elasticity after subjecting concrete specimens to FTC yielded ambiguous results. Structural damage could, however, be quantified through direct tensile tests and the subsequent determination of tensile strength, secant modulus of elasticity and fracture energy. The presented comparative analysis is restricted by the requirement of crack-predetermination through notching monolithic specimens. As the introduction of an epoxy coating successfully prevented freeze–thaw damage outside of the desired area, this procedure may serve to predetermine cracking in monolithic specimens without the need for notches. In this case, testing a larger number of monolithic specimens—partly notched—is recommended. Surface deterioration, as a standard procedure for the assessment of freeze–thaw damage, was not included in this article for the localization of the joint. Nonetheless, it can be a valuable method for assessing concrete surface quality before the addition of a second concrete layer. The presented test procedure can be easily adopted for other exposure causing internal structural damage, such as alkali-silica-reaction, expansive sulfate attacks or FTC in combination with deicing salts.

DATA AVAILABILITY STATEMENT

The data that support the findings of this study are available from the corresponding author upon reasonable request.

ORCID

Jan P. Höffgen https://orcid.org/0000-0003-1115-282X

REFERENCES

1. EN 206:2017-01. Concrete – specification, performance, production and conformity; German version EN 206:2013+A1: 2016; 2017.
2. Basheer PAM, Nolan É. Near-surface moisture gradients and in situ permeation tests. Construct Build Mater. 2001;15(2–3): 105–14. https://doi.org/10.1016/S0950-0618(00)00059-3
3. Raupach M, Orlowsky J. Erhaltung von Betonbauwerken: Baustoffe und ihre Eigenschaften. 1st ed. Wiesbaden: GWV Fachverlage GmbH; 2008 (in German).
4. Silfwerbrand J. Bonded concrete overlays - research needs. In: Marchand J, editor. 2nd international symposium on advances in concrete through science and engineering, Bagneux, France: RILEM Publications; 2006. p. 193–206.
5. Lenz P. Beton-Beton-Verbund: Potentiale für Schubfugen. Dissertation, Technische Universität München, München; 2012 (in German).

6. Silfwerbrand J, Paulsson J. Better bonding of bridge deck overlays: the Swedish experience. Concr Int. 1998;10:56–61.
7. Talbot C, Pigeon M, Beaupré D, Morgan DR. Influence of surface preparation on long-term bonding of shotcrete. ACI Mater J. 1994;91(6):560–6.
8. Beushausen H. Long-term performance of bonded concrete overlays subjected to differential shrinkage. PhD thesis, University of Cape Town, Cape Town; 2005.
9. Turatsinze A, Granju J-L, Sabathier V, Farhat H. Durability of bonded cement-based overlays: effect of metal fibre reinforcement. Mater Struct. 2005;38(3):321–7. https://doi.org/10.1007/BF02479297
10. Beushausen H, Alexander MG. Crack development in bonded concrete overlays subjected to differential shrinkage: a parameter study. In: Alexander MG, Beushausen H, Dehn F, Moyo P, editors. Concrete repair, rehabilitation and retrofitting, Balkema - Proceedings and monographs in engineering, water and earth sciences. Leiden: Taylor & Francis/Balkema; 2006. p. 3–1058.
11. Saucier F, Pigeon M. Durability of new-to-old concrete bondings. In: Malhotra VM, editor. Evaluation and rehabilitation of concrete structures and innovations in design: SP-128. Volume 1 Farmington Hills, MI: ACI; 1991. p. 689–705. https://doi.org/10.14359/2066
12. Li S, Geissert DG, Frantz GC, Stephens JE. Freeze-thaw bond durability of rapid-setting concrete repair materials. ACI Mater J. 1999;96(2):242–9.
13. Qian Y, Zhang D, Ueda T. Interfacial tensile bond between substrate concrete and repairing mortar under freeze-thaw cycles. J Adv Concrete Technol. 2016;14(8):421–32. https://doi.org/10.3151/jact.14.421
14. Zhu H, Fan J, Yi C, Ma H, Chen H, Shi J, et al. Characterization of freeze-thaw resistance of new-to-old concrete based on the ultrasonic pulse velocity method. J Test Eval. 2021;49(1):20190639. https://doi.org/10.1520/JTE20190639
15. Kara İB. Experimental investigation of the effect of cold joint on strength and durability of concrete. Arab J Sci Eng. 2021;46(11):10397–408. https://doi.org/10.1007/s13369-021-05400-5
16. Yang H, Lee H, Yang K, Ismail MA, Kwon S. Time and cold joint effect on chloride diffusion in concrete containing ggbfs under various loading conditions. Construct Build Mater. 2018;167:739–48. https://doi.org/10.1016/j.conbuildmat.2018.02.093
17. Yoo S-W, Kwon S-J. Effects of cold joint and loading conditions on chloride diffusion in concrete containing ggbfs. Construct Build Mater. 2016;115:247–55. https://doi.org/10.1016/j.conbuildmat.2016.04.010
18. Yoon Y, Yang K, Kwon S. Service life of ggbfs concrete under carbonation through probabilistic method considering cold joint and tensile stress. J Build Eng. 2020;32:101826. https://doi.org/10.1016/j.jobe.2020.101826
19. Nagataki S, Otsuki N, Moriwake A, Miyazato S, Shibata T. Macrocell corrosion on embedded bars in concrete members with joints. In Christer Sjostrom, editor, Durability of building materials and components 7. 1. London:Spon Press. 1996. p. 411–420.
20. Kobayashi K, Hattori A, Miyagawa T. Macro-cell corrosion of steel bars in self-compacting concrete. In: Banthia N, Sakai K, Gjorv OE, editors, Concrete under severe conditions (CONSEC'01): Proceedings. Vol. 2. Vancouver; 2001. p. 1368–75.
21. Barkey DP. Corrosion of steel reinforcement in concrete adjacent to surface repairs. ACI Mater J. 2004;4:266–72.
22. Skoglund P. Chloride transport and reinforcement corrosion in the vicinity of the transition zone between substrate and repair concrete. PhD thesis, KTH, Stockholm; 2007. https://www.diva-portal.org/smash/record.jsf?pid=diva2%3A11675&dswid=3061.
23. Skoglund P, Silfwerbrand J, Holmgren J, Trägårdh J. Chloride redistribution and reinforcement corrosion in the interfacial region between substrate and repair concrete—a laboratory study. Mater Struct. 2008;41(6):1001–14. https://doi.org/10.1617/s11527-007-9301-6
24. Lee M, Chiu C, Wang Y. The study of bond strength and bond durability of reactive powder concrete. ASTM Int. 2005;2(7):104–13.
25. Tayeh BA, Bakar BHA, Johari MAM, Voo YL. Mechanical and permeability properties of the interface between normal concrete substrate and ultrahigh performance fiber concrete overlay. Construct Build Mater. 2012;36:538–48. https://doi.org/10.1016/j.conbuildmat.2012.06.013
26. Stark J and Wicht B. Dauerhaftigkeit von Beton. Springer Vieweg, Berlin and Heidelberg, 2., aktualisierte und erweiterte Auflage; 2013. doi: https://doi.org/10.1007/978-3-642-35278-2. http://search.ebscohost.com/login.aspx?direct=true&scope=site&db=nlebk&db=nlabk&AN=669246 (in German).
27. BAW-Code of Practice MDCC. BAW code of practice: durability design and assessment of reinforced concrete structures exposed to carbonation and chlorides (MDCC). Karlsruhe: MDCC; 2019.
28. ASTM C1202–19. Test method for electrical indication of concretes ability to resist chloride ion penetration. West Conshohocken: ASTM International; 2019. https://doi.org/10.1520/C1202-19
29. EN 12390-11:2015-11. Testing hardened concrete – part 11: determination of the chloride resistance of concrete, unidirectional diffusion; 2015.
30. AASHTO T 259. Standard method of test for resistance of concrete to chloride ion penetration. Washington, DC: AASHTO T 259; 2017.
31. NT Build 443. Concrete, hardened: accelerated chloride penetration; 1995.
32. Cramer F. Mehrfeld-Modell für chemisch-physikalische Alterungsprozesse von Beton. Dissertation, Technische Universität Carolo-Wilhelmina zu Braunschweig, Braunschweig; 2015 (in German).
33. Fib Bulletin 34. Model code for service life design, volume 34 of Fib Bulletin. Fib, Lausanne; 2006. https://doi.org/10.35789/fib.BULL.0034.
34. Fagerlund G. Internal frost attack - state of the art: suggestions for future research. PhD thesis, Lund Institute of Technology, Lund, Sweden; 1997.
35. Setzer MJ. Frostschaden - Grundlagen und Prüfung. Beton- und Stahlbetonbau. 2002;97(7):350–9. https://doi.org/10.1002/best.200201620 (in German).
36. M. J. Setzer. Physikalische Grundlagen der Frostschädigung von Beton. In Müller HS, Nolting U, Haist M, editors. Dauerhafter Beton - Grundlagen, Planung und Ausführung bei Frost- und Frosttaumittel-Beanspruchung. 6. Symposium Baustoffe und Bauwerkserhaltung Universität Karlsruhe (TH); Karlsruhe, 12. März 2009, Volume 6. Symposium Baustoffe und Bauwerkserhaltung. KIT Scientific Publishing, Karlsruhe; 2009. p. 5–12 (in German).

37. M. Haist, Z. Djuric, and H. S. Müller. Betontechnologische Grundlagen zur Herstellung frostbeständiger Betone. In: Müller HS, Nolting U, Haist M, editors. Dauerhafter Beton - Grundlagen, Planung und Ausführung bei Frost und Frosttaumittel-Beanspruchung. 6. Symposium Baustoffe und Bauwerkserhaltung Universität Karlsruhe (TH); Karlsruhe, 12. März 2009, Volume 6. Symposium Baustoffe und Bauwerkserhaltung. KIT Scientific Publishing, Karlsruhe; 2009. p. 21–32 (in German).
38. CEN/TS 12390-9. Testing hardened concrete – part 9: freeze-thaw resistance with de-icing salts – scaling; German version CEN/TS 12390-9:2016; 2017.
39. CEN/TR 15177:2006-06. Testing the freeze-thaw resistance of concrete – internal structural damage; German version CEN/-TR 15177:2006; 2006.
40. Haufe J, Vollpracht A. Tensile strength of concrete exposed to sulfate attack. Cem Concr Res. 2019;116:81–8. https://doi.org/10.1016/j.cemconres.2018.11.005
41. Wiedmann AB. Schadensrisiko und Schadensentwicklung in Betonfahrbahndecken als Folge einer Alkali- Kieselsäure-Reaktion. Dissertation, Karlsruher Institut für Technologie, Karlsruhe; 2020 (in German).
42. EN12390-18:2021-09. Testing hardened concrete – part 18: determination of the chloride migration coefficient; German version EN 12390-18:2021; 2021.
43. Höffgen JP, Mohs M, Sonderegger E, Malárics-Pfaff V, Dehn F. Experimental methods for the analysis of the tensile behaviour of concrete joints. Struct Concr. 2022. https://doi.org/10.1002/suco.202200181
44. Dehghan A, Peterson K, Riehm G, Bromerchenkel LH. Application of x-ray microfluorescence for the determination of chloride diffusion coefficients in concrete chloride penetration experiments. Construct Build Mater. 2017;148:85–95. https://doi.org/10.1016/j.conbuildmat.2017.05.072
45. EN 12390-3:2019-10. Testing hardened concrete – part 3: compressive strength of test specimens; German version EN 12390-3:2019; 2019.
46. EN 12390-6:2010-09. Testing hardened concrete – part 6: tensile splitting strength of test specimens; German version EN 12390-6:2009; 2010.
47. EN 12390-13:2014-06. DIN EN 12390-13:2014-06, testing hardened concrete – part 13: determination of secant modulus of elasticity in compression; German version EN 12390-13:2013; 2014.

AUTHOR BIOGRAPHIES

Jan P. Höffgen
Institute of Concrete Structures and Building Materials, Karlsruhe Institute of Technology, Karlsruhe DE 76131, Germany
jan.hoeffgen@kit.edu

Matthias Mohs
Institute of Concrete Structures and Building Materials, Karlsruhe Institute of Technology, Karlsruhe DE 76131, Germany
matthias.mohs@baw.de

Sarah Lamparter
Institute of Concrete Structures and Building Materials, Karlsruhe Institute of Technology, Karlsruhe DE 76131, Germany
sarah.lamparter@kit.edu

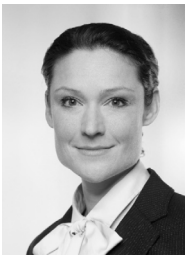

Viktória Malárics-Pfaff
Federal Waterways Engineering and Research Facility, Structural Engineering, Karlsruhe DE 76187, Germany
viktoria.malarics-pfaff@baw.de

Frank Dehn
Institute of Concrete Structures and Building Materials, Karlsruhe Institute of Technology, Karlsruhe DE 76131, Germany
frank.dehn@kit.edu

How to cite this article: Höffgen JP, Mohs M, Lamparter S, Malárics-Pfaff V, Dehn F. Experimental methods for the analysis of the durability behavior of concrete joints. Structural Concrete. 2022. https://doi.org/10.1002/suco.202200204